JOURNAL OF AIRCRAFT
Vol. 34, No. 1, January–February 1997

Matched Filter Concept and Maximum Gust Loads

Thomas A. Zeiler*
University of Alabama, Tuscaloosa, Alabama 35487-0280

In the course of NASA evaluations of the statistical discrete gust method for determining worst-case gust loads on aircraft, it was found that the concept of the matched filter from signal processing theory could be applied to the analysis of time-correlated, worst-case gust loads for mathematically linear aircraft models. Much of the work on the matched filter approach to gust loads analysis that followed had been geared toward a fundamental understanding of the implications of the matched filter theory interpretation of the gust loads analysis problem, as well as various attempts at extending the techniques to nonlinear aircraft models. A rigorous development of the matched filter interpretation of gust loads within the context of the theory of random processes is presented and includes discussion of its relationship to existing statistically based methods for the calculation of design gust loads for linear aircraft. It is shown, using the matched filter theory formalism, that the load peak-to-rms ratio can be related to the energy of the matched excitation waveform. Also, it is shown that a candidate design value of the peak-to-rms ratio that has been reported in the literature to be around 3 may have its basis in the discretization process that accompanies both data reduction and stochastic simulation on digital computers.

Nomenclature

$A[\,]$ = temporal average
$\bar{A}$ = load-rms-to-gust-rms ratio, Eq. (33)
$E[\,]$ = ensemble average
$G(\omega)$ = gust frequency response function
$H(\omega)$ = system frequency response function
$h(t)$ = unit impulse response
K = arbitrary constant, Eq. (3)
$P(y)$ = cumulative probability distribution of random variable y
$p(y)$ = probability density function of random variable y
$R(\tau)$ = correlation function
t, T = time variable, interval
$U_{x,T}$ = energy of waveform $x(t)$ over time interval T
U_σ = design gust velocity
Z = partition, Eq. (17)
z = normalized maximum variable
Δ = increment
$\delta(\,)$ = Dirac delta function
ζ = normalized load
η_d = load peak-to-rms factor
ρ = correlation coefficient
σ = standard deviation
τ = time
$\Phi_g(\omega)$ = power spectral density of atmospheric turbulence
ψ = normalized load
ω = circular frequency, rad/s

Introduction

IN the late 1980s, the Federal Aviation Administration (FAA) requested assistance from the National Aeronautics and Space Administration (NASA) for initial evaluation of a candidate method for analysis of gust loads on aircraft with nonlinearities. The candidate method, known as the statistical discrete gust (SDG) method,[1] promised to permit analysis of mathematically nonlinear aircraft models for worst-case gust loads and be equivalent to existing methods for mathematically linear aircraft models. Being a time-domain method, it would also permit the computation of time-correlated loads. NASA conducted the evaluation of the SDG method, focusing on its overlap with the existing linear methods.[2] In the course of these studies, it was found that the concept of the matched filter from signal processing theory[3,4] could be applied to the analysis of time-correlated, worst-case gust loads for mathematically linear aircraft models. Much of the work on the matched filter approach to gust loads analysis that followed had been geared toward a fundamental understanding of the implications of the matched filter theory interpretation of the gust loads analysis problem, as well as various attempts at extending the techniques to nonlinear aircraft models. Ultimately, the desire has been to develop an accurate, reliable, and inexpensive technique for the determination of maximum gust loads on mathematically nonlinear aircraft. It is felt that a deeper understanding of the linear case, abstracted to fundamental principles, will better guide the development of techniques for the nonlinear case.

A good deal of the work on what has come to be known as the matched filter theory (MFT) approach to the analysis of maximum and time-correlated gust loads has been documented in various papers and presentations.[3,5–8] This paper presents a rigorous development of the matched filter interpretation of gust loads within the context of the theory of random processes, and includes discussion of its relationship to existing statistically based methods for the calculation of design gust loads for linear aircraft.

Mathematical Development

Linear System Response

The response $y(t)$ of a linear system with unit impulse response $h_y(t)$ to an arbitrary excitation $x(t)$ can be expressed by the Duhamel or convolution integral:

$$y(t) = \int_{-\infty}^{+\infty} h_y(t - t')x(t')\,dt' = \int_{-\infty}^{t} h_y(t - t')x(t')\,dt' \qquad (1)$$

Received July 16, 1996; revision received Oct. 10, 1996; accepted for publication Oct. 17, 1996.

*Assistant Professor, Department of Aerospace Engineering and Mechanics. Senior Member AIAA.

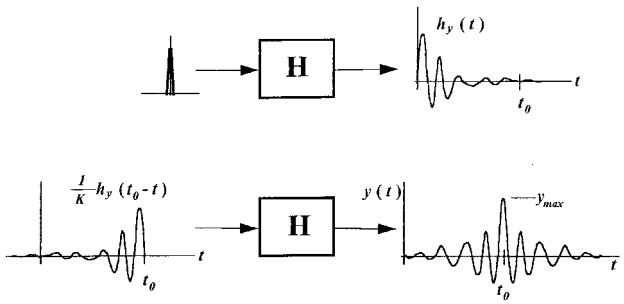

Fig. 1 Maximum response of a linear system.

The upper bound of the maximum magnitude of the response at some time $t = t_0$, is expressed by Schwartz's inequality:

$$|y(t_0)|^2 = \left| \int_{-\infty}^{t_0} h_y(t - t')x(t')\,dt' \right|^2$$

$$\leq \left| \int_{-\infty}^{t_0} h_y^2(t_0 - t')\,dt' \right| \left| \int_{-\infty}^{t_0} x^2(t')\,dt' \right| \tag{2}$$

The equality in Eq. (2) holds if, for any K

$$x(t) = \tilde{x}(t) = (1/K)h_y(t_0 - t) \tag{3}$$

Hence, $\tilde{x}(t)$ is the required excitation to produce a maximum response of the system at time $t = t_0$. Note that it is proportional to the unit impulse response shifted and reversed in time. This concept is sketched in Fig. 1. In Ref. 3, this sample is referred to as the matched excitation waveform, since it is derived from, or matched to, the impulse response of the combined turbulence/aircraft-load filter through Eq. (3). The maximum response is then

$$|y(t_0)|_{\max} = \frac{1}{|K|} \left| \int_{-\infty}^{t_0} h_y^2(t_0 - t)\,dt \right| = \frac{1}{|K|} \left| \int_{-\infty}^{\infty} h_y^2(t_0 - t)\,dt \right| \tag{4}$$

Since the integrand is always positive, then for any time $t < t_0$, $|y(t)|_{\max} < |y(t_0)|_{\max}$. Although the lower integral limit is $-\infty$, a typical system might be sufficiently damped so that most of the pertinent dynamics of the system are contained in the early part of the impulse response. Therefore, t_0 can be chosen so that most of the energy content of the impulse response is contained within the time interval $0 \leq t \leq t_0$, rendering finite time and frequency integrals reasonably accurate approximations to the infinite time and frequency integrals. While this sacrifices some mathematical generality, it does present practical implementation advantages.

The integral in Eq. (4) may be evaluated by applying Parseval's theorem, where $H_y(\omega)$ is the frequency response function of the linear system

$$\int_{-\infty}^{+\infty} h_y^2(t_0 - t)\,dt = \frac{1}{2\pi} \int_{-\infty}^{+\infty} H_y^*(\omega)e^{-i\omega t_0}H_y(\omega)e^{i\omega t_0}\,d\omega$$

$$= \frac{1}{2\pi} \int_{-\infty}^{+\infty} H_y^*(\omega)H_y(\omega)\,d\omega \tag{5}$$

which is the mean square of the response of the system to a unit white noise excitation. If the excitation has a zero mean, this is also known as the variance, $\sigma_{h_y}^2$. We shall be assuming from here on that all processes under consideration have zero mean unless otherwise stated. The superscript asterisk in Eq. (5) denotes the complex conjugate. Thus, the maximum response of the system is

$$|y(t_0)|_{\max} = \sigma_{h_y}^2/|K| \tag{6}$$

The matched filter, as originally conceived, is an electronic filter designed so that its response to a known input signal is maximum at a specific time.[4,9–11] It found early application to radar with the filter taken to be a detector that, in response to a known incoming radar signal $\tilde{x}(t)$, produces an output signal with maximized signal-to-noise ratio. The unit impulse response function of such a filter is

$$h_y(t) = K\tilde{x}(t_0 - t) \tag{7}$$

which is the so-called matched filter solution. Equations (3) and (7) are just alternate forms of the same principle.

Both forms present useful interpretations within the context of the application of MFT to the problem of determining maximum, time-correlated gust loads on aircraft. We model atmospheric turbulence as a continuous random process, and consider a gust to be a particular sample or realization of this turbulence. Further, we may think of the turbulence as being representable as a linear filter responding to a zero-mean unit Gaussian white noise excitation. Hence, the turbulence is Gaussian colored noise, and an aircraft's load response to turbulence is equivalent to the response of the second filter to the colored noise. Since the turbulence and aircraft load response filters can be combined into a single filter, the load response is then the response of the combined filter to unit Gaussian white noise. The critical gust profile, which produces the maximum load response, is the response of the turbulence filter to a particular sample or realization of the white noise. This particular sample of the white noise excitation is given by Eq. (3). Our understanding of the problem is not yet complete because of the K in Eq. (3). In earlier treatments of the matched filter principle applied to gust loads, this constant was set equal to the square root of the variance, $\sigma_{h_y}^2$. This is unnecessarily restrictive, and can lead to confusion if the system being excited is nonlinear. We may address the constant by considering in detail the statistical characteristics of a sample of a zero-mean Gaussian white noise random process following Stratonovich.[12]

Energy of a Sample of White Noise

Consider a stationary, ergodic, zero-mean Gaussian white noise process $x_w(t)$ of variance σ_w^2. For unit white noise, the variance is unity. The autocorrelation of the process is

$$R(t' - t) = \lim_{T\to\infty} \frac{1}{2T} \int_{-T}^{T} x_w(t)x_w(t')\,dt' = A[x_w(t)x_w(t')]$$

$$= E[x_w(t)x_w(t')] = \sigma_w^2\delta(t - t') \tag{8}$$

where $A[\,]$ and $E[\,]$ are both forms of the expected value, and $\delta(t - t')$ is the Dirac delta, or unit impulse function. It is the property of ergodicity that makes temporal and ensemble averages equal. Consider a particular realization of this process, as displayed in Fig. 2, and imagine that a sample of this realization of a finite time duration is subdivided into N equal time slices of duration Δt with divisions at $t_1, t_2, \ldots, t_j, \ldots$.

The mean value of $x_w(t)$ over time segment j is then

$$\bar{x}_j = A[x_w(t)]_{\Delta t} = \frac{1}{\Delta t} \int_{t_j - \Delta t}^{t_j} x_w(t)\,dt \tag{9}$$

These temporal means $\bar{x}_j$ are also zero-mean random quantities with variance

$$E(\bar{x}_i\bar{x}_j) = E\left[\frac{1}{(\Delta t)^2} \int_{t_i - \Delta t}^{t_i} x_w(t)\,dt \int_{t_j - \Delta t}^{t_j} x_w(t')\,dt' \right] \tag{10}$$

Note that even though each mean is determined as a temporal average over a small finite time, Eq. (10) is an average of the

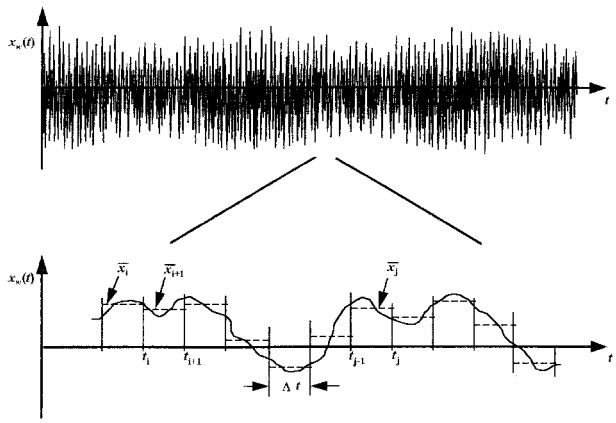

Fig. 2 Hypothetical sample of a white noise random process.

products of all such samples of temporal averages, and is thus an ensemble average. Rearranging the integrals

$$E(\bar{x}_i\bar{x}_j) = E\left[\frac{1}{(\Delta t)^2}\int_{t_i-\Delta t}^{t_i}\int_{t_j-\Delta t}^{t_j} x_w(t)x_w(t')\,dt\,dt'\right] \tag{11}$$

Moving the expected value operator inside the integrals and using the expected value from Eq. (8)

$$E(\bar{x}_i\bar{x}_j) = \frac{1}{(\Delta t)^2}\int_{t_i-\Delta t}^{t_i}\int_{t_j-\Delta t}^{t_j} \sigma_w^2\delta(t-t')\,dt\,dt' \tag{12}$$

Noting that the time variable t can become equal to the time variable t' only when i equals j

$$E(\bar{x}_i\bar{x}_j) = \frac{1}{(\Delta t)^2}\int_{t_i-\Delta t}^{t_i} \sigma_w^2\,dt' = \frac{\sigma_w^2}{\Delta t} \tag{13}$$

The $\bar{x}_j$ are also Gaussian, and so have the probability density

$$p(\bar{x}_j) = \left(\frac{1}{\sqrt{2\pi\sigma_w^2/\Delta t}}\right)\exp\left(-\frac{\bar{x}_j^2}{2\sigma_w^2}\Delta t\right) \tag{14}$$

Considered collectively, N segments of duration Δt, spanning a total time from $t = \tau$ to $t = \tau + T$, have a joint probability density of

$$p(\bar{x}_1, \bar{x}_2, \ldots, \bar{x}_j, \ldots, \bar{x}_N) = \left(\frac{1}{\sqrt{2\pi\sigma_w^2/\Delta t}}\right)^N \exp\left(-\frac{1}{2\sigma_w^2}\sum_{j=1}^{N}\bar{x}_j^2\Delta t\right) \tag{15}$$

which, in the limit, becomes

$$p[x_w(t), T] = \lim_{N\to\infty} p(\bar{x}_1, \bar{x}_2, \ldots, \bar{x}_j, \ldots, \bar{x}_N) = \frac{1}{Z}\exp\left[-\frac{1}{2\sigma_w^2}\int_\tau^{\tau+T} x_w^2(t)\,dt\right] \tag{16}$$

This is the probability density for the infinite sequence of values of the function $x_w(t)$ within the time interval $\tau \le t \le \tau + T$. In essence, it is the probability density of realizations of the function over the time interval, rather than of discrete values of the function, as we are perhaps used to thinking of the probability density of a random process. Being a probability density, its integral over all possible $x_w(t)$ should be unity. Hence, the weighting, or partition Z, may be expressed as

$$Z = \lim_{N\to\infty}\int_{\bar{x}_N=-\infty}^{+\infty}\cdots\int_{\bar{x}_j=-\infty}^{+\infty}\cdots\int_{\bar{x}_2=-\infty}^{+\infty}\int_{\bar{x}_1=-\infty}^{+\infty} \times \exp\left(-\frac{1}{2\sigma_w^2}\sum_{j=1}^{N}\bar{x}_j^2\Delta t\right)(d\bar{x}_1\,d\bar{x}_2\cdots d\bar{x}_j\cdots d\bar{x}_N) = \int_{x_w(t)}\exp\left[-\frac{1}{2\sigma_w^2}\int_\tau^{\tau+T}x_w^2(t)\,dt\right]dx_w(t) \tag{17}$$

The integral in the exponential term of the probability density can be thought of as an energy measure

$$U_{x,T} = \int_\tau^{\tau+T} x_w^2(t)\,dt \tag{18}$$

Then Eq. (16) becomes

$$p[x_w(t), T] = \frac{1}{Z}\exp\left(-\frac{U_{x,T}}{2\sigma_w^2}\right) \tag{19}$$

The probability of encountering some waveform $x(t)$ of energy U or less over the time interval $\tau \le t \le \tau + T$ would then be the integral of Eq. (19) over the subspace of functions $x_w(t)$ with energy U or less over the time interval $\tau \le t \le \tau + T$.

Therefore, if the matched excitation waveform, Eq. (3), is in a sample of unit white noise

$$\int_\tau^{\tau+t_0}\tilde{x}^2(t)\,dt = \frac{1}{K^2}\int_\tau^{\tau+t_0}h_y^2(t_0-t)\,dt = \tilde{U}_{x,t_0} \tag{20}$$

Recalling Eq. (5), then

$$\tilde{U}_{x,t_0} = \sigma_{h_y}^2/K^2 \tag{21}$$

the matched excitation waveform is

$$\tilde{x}(t) = (\sqrt{\tilde{U}_{x,t_0}}/\sigma_{h_y})h_y(t_0-t) \tag{22}$$

and the maximum response of the system is

$$|y|_{\max} = \sqrt{\tilde{U}_{x,t_0}}\sigma_{h_y} \tag{23}$$

The preceding derivation shows that, for all excitation waveforms of a given energy over a specified time interval [satisfying Eq. (20)], the maximum response of the linear system is given by Eq. (23), and is a result of a matched excitation waveform possessing that energy within the time interval $\tau \le t \le \tau + t_0$. Any waveform of less energy, and thus more likely to occur, will produce a maximum response that is lower. However, it is possible for a waveform of greater energy to produce a response equal to (or greater than) the maximum response in the time interval, but such a waveform is less likely since it is of greater energy. Hence, an alternative interpretation of the matched filter principle may be stated: of all the waveforms most likely to occur above a certain level of probability within a Gaussian white noise excitation of a linear system, the matched excitation waveform is the one that produces a maximum response of the linear system.

Phased Design Loads Analysis and the Matched Filter

$H_y(\omega)$ has been used to describe the response of a linear system to zero-mean, unit Gaussian white noise. Within the context of flight vehicle structural load response to atmo-

spheric turbulence, we generally have available the frequency response function relating a load response to turbulence $\tilde{H}_y(\omega)$. We may define turbulence as the response of a linear filter to zero-mean, unit Gaussian white noise. A frequency response function for the turbulence filter may be introduced so that

$$H_y(\omega) = \tilde{H}_y(\omega)G(\omega) \tag{24}$$

Note then that we may define σ_g as the square root of the variance of the response of the turbulence filter to zero mean, unit Gaussian white noise. Hence, it is also the rms of the turbulence velocity.

Again, some response, $y(t)$, of a linear system to the corresponding matched excitation waveform

$$\tilde{x}_y(t) = (\sqrt{U_{x_y x_0}}/\sigma_{h_y})h_y(t_0 - t)$$

can be written as a convolution integral

$$\begin{aligned} y(t) &= \int_{-\infty}^{+\infty} h_y(t - t')\tilde{x}_y(t')\,dt' \\ &= \frac{\sqrt{U_{x_y x_0}}}{\sigma_{h_y}} \int_{-\infty}^{+\infty} h_y(t - t')h_y(t_0 - t')\,dt' \end{aligned} \tag{25}$$

Recognizing Fourier transform pairings and rearranging the order of integration

$$\begin{aligned} y(t) &= \frac{\sqrt{U_{x_y x_0}}}{\sigma_{h_y}} \int_{-\infty}^{+\infty} h_y(t - t') \left[\frac{1}{2\pi} \int_{-\infty}^{+\infty} H_y^*(\omega) e^{i\omega t'} e^{-i\omega t_0}\,d\omega \right] dt' \\ &= \frac{\sqrt{U_{x_y x_0}}}{\sigma_{h_y}} \left[\frac{1}{2\pi} \int_{-\infty}^{+\infty} H_y^*(\omega)H_y(\omega) e^{i\omega(t - t_0)}\,d\omega \right] \\ &= \frac{\sqrt{U_{x_y x_0}}}{\sigma_{h_y}} R_{yy}(t - t_0) \\ &= \sigma_{h_y}\sqrt{U_{x_y x_0}}\rho_{yy}(t - t_0) \end{aligned} \tag{26}$$

where $R_{yy}(t - t_0)$ is the autocorrelation function for the response $y(t)$, and $\rho_{yy}(t - t_0)$ is the autocorrelation coefficient that equals unity when $(t - t_0) = 0$. By a similar procedure, we may find the response of some other output quantity $z(t)$, considering the linear system to be multioutput, to the same excitation waveform to be

$$z(t) = (\sqrt{U_{x_y x_0}}/\sigma_{h_y})R_{zy}(t - t_0) = \sigma_{h_z}\sqrt{U_{x_y x_0}}\rho_{zy}(t - t_0) \tag{27}$$

where $R_{zy}(t - t_0)$ and $\rho_{zy}(t - t_0)$ are the cross-correlation function and cross-correlation coefficient between outputs $y(t)$ and $z(t)$, respectively. Usually, the value of $\rho_{zy}(t - t_0)$ at $(t - t_0) = 0$ is referred to simply as the correlation coefficient ρ_{zy}, and has magnitude less than or equal to unity. We see from the previous derivations that responses of a linear system to a matched excitation waveform are proportional to auto- and cross-correlations, and that the amplitudes vary directly with the square root of the variance of the output in question and the square root of the energy of the excitation waveform.

Now the bivariate, or joint, Gaussian probability density function (PDF) for the responses, $y(t)$ and $z(t)$, to zero-mean unit white noise excitation is

$$p(y, z) = \frac{1}{2\pi\sigma_{h_y}\sigma_{h_z}\sqrt{1 - \rho_{zy}^2}} \times \exp\left[-\frac{\left(\frac{y^2}{\sigma_{h_y}^2} - 2\rho_{zy}\frac{yz}{\sigma_{h_y}\sigma_{h_z}} + \frac{z^2}{\sigma_{h_z}^2} \right)}{2(1 - \rho_{zy}^2)} \right] \tag{28}$$

If the numerator of the exponential were to be held constant, then one would have an equation for an ellipse

$$\frac{y^2}{\sigma_{h_y}^2} - 2\rho_{zy}\frac{yz}{\sigma_{h_y}\sigma_{h_z}} + \frac{z^2}{\sigma_{h_z}^2} = C$$

and all combinations of y and z that reside on the ellipse have the same probability density and are thus equally probable. When one quantity, say y, is at its maximum value, the other is at its maximum value times the correlation coefficient

$$\frac{y_{\max}^2}{\sigma_{h_y}^2} - 2\rho_{zy}^2\frac{y_{\max}z_{\max}}{\sigma_{h_y}\sigma_{h_z}} + \rho_{zy}^2\frac{z_{\max}^2}{\sigma_{h_z}^2} = C$$

The maximum values are equal to a factor times the square root of the corresponding zero-mean rms

$$y_{\max} = \eta_d\sigma_{h_y} \tag{29a}$$

$$z_{\max} = \eta_d\sigma_{h_z} \tag{29b}$$

Then the constant C may be found as $\eta_d^2(1 - \rho_{zy}^2)$.

In the analysis of turbulence design loads, the factor η_d is the ratio of a peak design load to the rms value. If the ellipse equation is divided by η_d, we may define normalized load responses

$$\psi = y/\eta_d\sigma_{h_y} \quad \text{and} \quad \zeta = z/\eta_d\sigma_{h_z}$$

so that

$$\psi^2 - 2\rho_{zy}\psi\zeta + \zeta^2 = (1 - \rho_{zy}^2) \tag{30}$$

describes a normalized design loads ellipse that is independent of the actual load magnitude, with its shape dependent upon the correlation coefficient. Also, since we have been dealing only with linear systems excited by zero-mean loading, we should make note of the fact that these loads are typically in addition to steady state, 1-G loads experienced by the aircraft in trimmed flight. The total design loads are then

$$Y_{\text{des}} = Y_{1-G} \pm \eta_d\sigma_{h_y} \quad \text{and} \quad Z_{\text{des}} = Z_{1-G} \pm \eta_d\sigma_{h_z}$$

or, when normalized

$$\Psi_{\text{des}} = Y_{\text{des}}/\eta_d\sigma_{h_y} = \Psi_{1-G} \pm 1 \quad \text{and} \quad Z_{\text{des}} = Z_{\text{des}}/\eta_d\sigma_{h_y} = \Psi_{1-G} \pm 1$$

A typical normalized loads diagram is shown in Fig. 3. While the incremental turbulence loads are independent of the turbulence magnitude when the normalization is employed, the location of the center of the equiprobable loads ellipse in Fig. 3 is not dependent upon the characteristics of the system's response to turbulence. For different weight or flight condi-

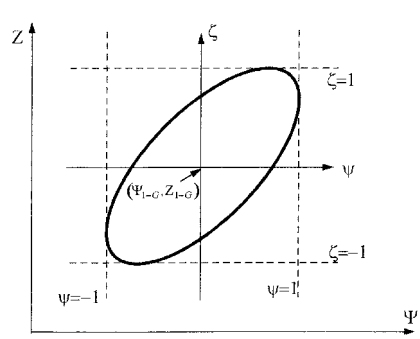

Fig. 3 Normalized 1-G plus phased design loads for turbulence.

tions or different turbulence intensities (rms), the rms loads may be different. Hence, the location in Fig. 3 of the nondimensionalized 1-G loads will vary from one condition to another.

When the responses to a matched excitation waveform [Eqs. (25) and (26)], are normalized as

$$\psi(t) = y(t)/(\eta_d \sigma_{h_y}) \quad \text{and} \quad \zeta(t) = z(t)/(\eta_d \sigma_{h_z})$$

and plotted on an equiprobable loads ellipse as parametric functions of time, the result is a plot such as shown conceptually in Fig. 4. The arrows indicating the direction of increasing time and corresponding plots of the two loads quantities vs time are also shown. The load plot will be tangent to the ellipse at a point with the load coordinates of unity and ρ_{zy}. Which of the two loads is unity and which is the correlation coefficient depends upon which response quantity the matched excitation waveform is matched to. In Fig. 4, the excitation is obviously matched to ζ. Typically, such parametric load plots won't be so distinct as in Fig. 4, and will have more the appearance of those shown in Fig. 5. Figures 5a and 5b show a case in which the correlation coefficient is fairly large. This results in a slender ellipse. A correlation coefficient of unity would result in an ellipse degenerated to a straight line, whereas a correlation coefficient of zero would produce a circle. Figures 5c and 5d show a case for which the correlation coefficient is fairly small and also negative.

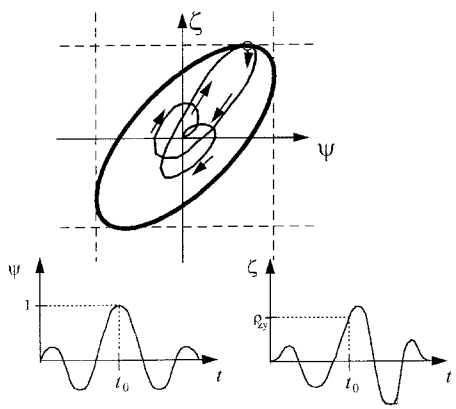

Fig. 4 Normalized equiprobable design loads ellipse with parametric loads plot.

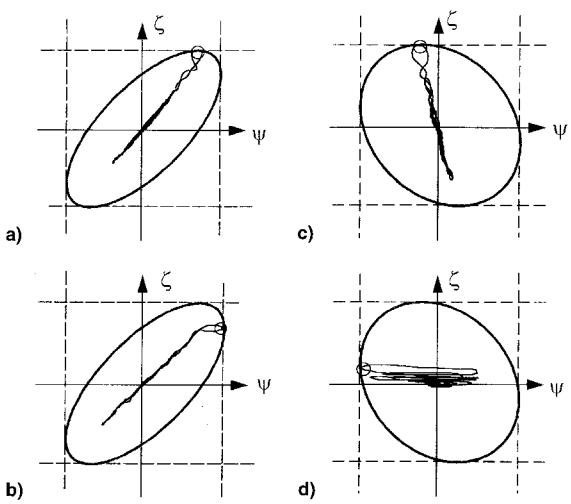

Fig. 5 Normalized parametric load plots with normalized design loads ellipses. a) ζ-matched excitation waveform, $\rho_{xy} = 0.75$; b) ψ-matched excitation waveform, $\rho_{xy} = 0.75$; c) ζ-matched excitation waveform, $\rho_{xy} = -0.2$; and d) ψ-matched excitation waveform, $\rho_{xy} = -0.2$.

Comparing Eq. (23) with Eqs. (29a) and (29b), we see that the peak load-to-rms ratio is related to the excitation waveform energy by

$$\sqrt{\tilde{U}_{x_y,t_0}} = \sqrt{\tilde{U}_{x_z,t_0}} = \sqrt{\tilde{U}_{x,t_0}} = \eta_d \tag{31}$$

It is common practice to characterize an rms gust load response as a product of the rms gust velocity and an rms ratio, called A-bar

$$\sigma_{h_y} = \bar{A}_y \sigma_g \tag{32}$$

$$\bar{A}_y = \frac{\sigma_{h_y}}{\sigma_g} = \frac{\dfrac{1}{2\pi}\displaystyle\int_{-\infty}^{+\infty} H_y^*(\omega) H_y(\omega)\, d\omega}{\dfrac{1}{2\pi}\displaystyle\int_{-\infty}^{+\infty} G^*(\omega) G(\omega)\, d\omega}^{1/2}$$

$$= \frac{\dfrac{1}{2\pi}\displaystyle\int_{-\infty}^{+\infty} \Phi_g(\omega) \tilde{H}_y^*(\omega) \tilde{H}_y(\omega)\, d\omega}{\dfrac{1}{2\pi}\displaystyle\int_{-\infty}^{+\infty} \Phi_g(\omega)\, d\omega}^{1/2} \tag{33}$$

The function $\Phi_g(\omega) = G^*(\omega)G(\omega)$ is the power spectral density of the atmospheric turbulence. Again, because linear systems are involved, this ratio characterizes the rms response to a turbulence of any intensity.

The bivariate PDF becomes

$$p(y, z) = \frac{1}{2\pi \bar{A}_y \bar{A}_z \sigma_g^2 \sqrt{1 - \rho_{zy}^2}} \times \exp\left[-\frac{\left(\dfrac{y^2}{\sigma_g^2 \bar{A}_y^2} - 2\rho_{zy} \dfrac{yz}{\sigma_g^2 \bar{A}_y \bar{A}_z} + \dfrac{z^2}{\sigma_g^2 \bar{A}_z^2} \right)}{2(1 - \rho_{zy}^2)} \right] \tag{34}$$

One method in use in the aircraft industry for establishing absolute levels for design loads is the design envelope criterion, wherein U_σ is defined such that the design loads are

$$Y_{\text{des}} = Y_{1-G} \pm U_\sigma \bar{A}_y \tag{35a}$$

$$Z_{\text{des}} = Z_{1-G} \pm U_\sigma \bar{A}_z \tag{35b}$$

The design gust velocity is stipulated by regulation[13] as a function of altitude and several of the standard design flight speeds.

The normalized loads for the equiprobable loads design ellipse become

$$\psi(t) = y(t)/(U_\sigma \bar{A}_y) \quad \text{and} \quad \zeta(t) = z(t)/(U_\sigma \bar{A}_z)$$

and the design gust velocity can be related to the matched excitation waveform energy by

$$U_\sigma = \sigma_g \sqrt{\tilde{U}_{x,t_0}} \tag{36}$$

and to the peak load-to-rms ratio by

$$\eta_d = U_\sigma / \sigma_g = \sqrt{\tilde{U}_{x,t_0}} \tag{37}$$

Thus, the selection of a design gust velocity is equivalent to the selection of a level of probability of the design loads, and corresponds to a matched excitation waveform of energy $\tilde{U}_{x,t_0}$. As described by Moon,[14] the load combinations that reside on

the ellipse are referred to as phased design loads. Since an infinity of combinations exists, typical practice is to circumscribe the loads ellipse by an octagon, and use the load combinations at each of the eight corners in strength analyses.

Determining Peak Loads Through Stochastic Simulation

While the design gust intensities discussed previously effectively establish the required peak load-to-rms ratio η_d for linear aircraft, they may not be applicable to aircraft with nonlinearities. Such nonlinearities might be spoilers used as load alleviation devices (their deployment is one-sided), saturation of rate-limited actuators, control surfaces with deflection limits, or inherently nonlinear aerodynamic loads. There has been some concern over an appropriate value for η_d in such cases. Aircraft that have had significant nonlinearities present have been handled on a case-by-case basis,[15,16] with stochastic simulation figuring prominently in the evaluations. Several attempts[15–17] at determining an appropriate value for η_d seem to suggest that the appropriate number is near 3.0. Further, Ref. 8 included results from stochastic simulations of both linear and nonlinear aircraft models, and found roughly the same factor to be applicable, although a certain amount of tuning of simulation times was done. This section of this article presents a simplified model of the expected maximum values in the results of a stochastic simulation of a linear system. It provides a formal background for interpreting simulation results that search for maximum responses, and could serve as a starting point in any developments for nonlinear systems.

The specifics of the method by which the results of Ref. 8 were obtained are of interest. Stochastic simulations of an aircraft load response to atmospheric turbulence were conducted. Out of the simulation results, samples of the load response with a (positive) maximum in the center of the sample were extracted from the simulation results and averaged. The time spans of the samples were twice the typical values of t_0 from the matched filter approach, i.e., the time for a linear system's impulse response to damp out to near zero. The resulting extracted–averaged traces of the load response were found to bear a striking resemblance to a linear matched response. The energy $\tilde{U}_{x_y,t_0}$ for the matched response calculation was set to unity and it was found that the extracted-averaged maximum response was about three times the maximum matched response. This factor varied somewhat, depending upon the time span of the extracted samples. The relative lengths of the extracted sample time spans and the overall simulation length has a secondary effect in that all of the samples were taken from the full simulation. Hence, the full simulation approximates the true random process, provided the sample time spans are sufficiently small by comparison.

When using digital computers to simulate the response of a dynamic system to a continuous random excitation, the process becomes a discrete time function composed of random values taken, or sampled, at discrete time intervals. Provided the full simulation time span is long enough and the sample time spans are small by comparison, the average maximum response is not dependent upon the simulation time span so much as it is upon the number of discrete time steps used. The size of the time step is typically driven by the highest system frequency that the analyst wants faithfully represented. The length of the simulation might then be driven by the typical length of time that the physical random excitation being modeled tends to persist in actual experience.

We may determine the expected value of the peak in a digital simulation of a continuous random process by considering the theory of extremal distributions in sets of samples composed of a finite number of discrete random events.[18] Given a sample composed of a sequence of n discrete events of a random process, the probability that one of the events is the largest at certain level Y is the same as the probability that all of the events in the sample are less than or equal to the value Y. If the process is described by $p(y)$, then the probability that any one event y_i is less than or equal to Y is then

$$P_i(y_i \leq Y) = \int_{-\infty}^{Y} p(y)\, dy \tag{38}$$

Hence, the probability that all of the events in the sample are less than or equal to Y (or the probability that Y is the largest value in the sample) is the product of the individual probabilities. If the events are uncorrelated, then

$$P(y_{\max} = Y) = \prod_{i=1}^{n} P_i(y_i \leq Y) = [P(y \leq Y)]^n \tag{39}$$

and the probability density is

$$p_Y(Y) = \frac{dP(y_{\max} = Y)}{dy} = n[P(y \leq Y)]^{n-1} p(y = Y) \tag{40}$$

and the expected value of the maximum Y is

$$E(Y) = \int_{-\infty}^{+\infty} Y p_Y(Y)\, dY \tag{41a}$$

or

$$E(z) = \int_{-\infty}^{+\infty} z p_Y(Y = \sigma_y z + \bar{y})\, dz = \bar{z} \tag{41b}$$

where

$$z = (Y - \bar{y})/\sigma_y$$

and $\bar{y}$ and σ_y^2 are the mean and variance of the basic random variable y. Taking $p(y = Y)$ to be a Gaussian probability density, the previous integral may be evaluated and is shown plotted in Fig. 6. Also shown is the result of evaluating the integral of Eq. (41b) using limits of ± 4 rather than $\pm\infty$. Numerical random number generators do not, of course, give exact representations of the intended random process, being least accurate at the extremes, or so-called tails, of the distributions. The expected values of the maxima, Eq. (41b), for integral limits of ± 4 fall below the exact expected values for $\pm\infty$, and actually begin to decrease rather than monotonically increase as n increases. This gives an indication of what one might obtain by counting maxima from stochastic simulations that use numerical random number generators. The lesson here is that such operations may underpredict extrema. Further, while individual points in a white noise excitation are uncorrelated, the points in the resulting response of a physical system are correlated. Physically this means that, given any particular

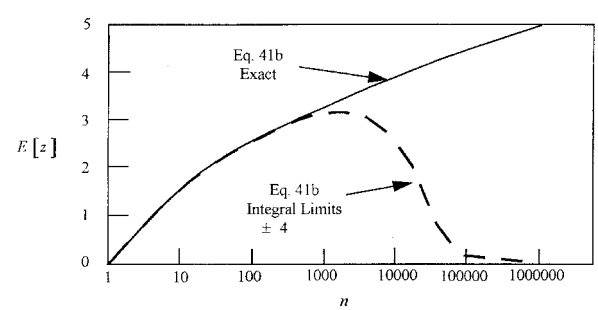

Fig. 6 Average maximum value of n Gaussian-distributed quantities vs n for different integral limits.

value of the response at one instant, the value of the response at some time interval later is limited by the natural dynamics of the system. This effect would limit the reachable maxima. While this is a worthy topic for further investigation, it is beyond the scope of this paper. The combined effects of numerical approximation and system dynamics may well be the influences in a figure from Ref. 8, shown reproduced in Fig. 7, along with results of applying Eq. (41b) for different time step sizes and, hence, different numbers of steps since $n = 2t_0/\Delta t$. Also, from Ref. 8 are shown range bars indicating the largest maximum in the 450-s simulation time as well as the smallest maxima for the pertinent sample times.

The variance of the maxima, Eq. (41b), is found from

$$\sigma_z^2 = \int_{-\infty}^{+\infty} (z - \bar{z})^2 p_Y(Y = \sigma_Y z + \bar{Y})\, dz \qquad (42)$$

and $\bar{z}$ and σ_z (standard deviation) are plotted together in Fig. 8. What we see is that the standard deviation decreases as the number n increases. Hence, the probability density function of the maxima becomes sharper as n increases and gradually more skewed, as shown in Fig. 9. Then, as n increases, the average maximum becomes a better estimate of the likely maximum that will be encountered in any circumstance since a given small region centered on the average value accounts for an increasing share of the total probability (integral of the density). That is, the actual maximum is increasingly likely to be encountered within a given small range. For a reasonably high

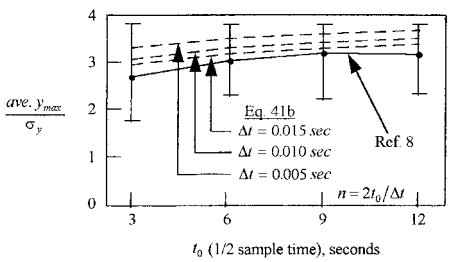

Fig. 7 Average maxima from Eq. (41b) and stochastic simulation, from Ref. 8.

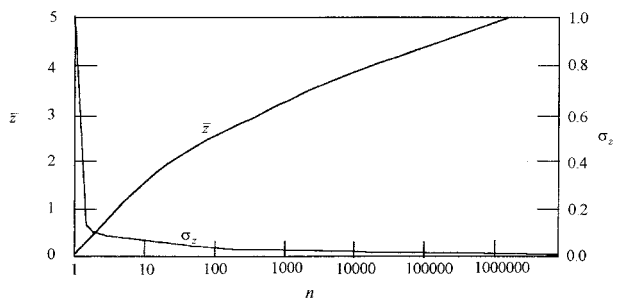

Fig. 8 Average and standard deviation of maxima vs number of samples or time steps.

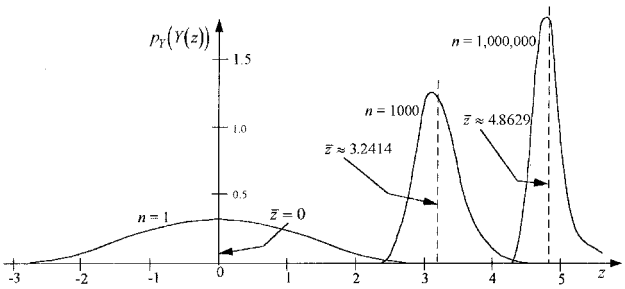

Fig. 9 Evolution of maxima probability densities with n.

number of time steps, one can feel confident that the likely maximum peak load is accounted for in a simulation.

Thus, for linear systems, one possible choice for the design load peak-to-rms ratio is given by

$$\eta_d = U_\sigma/\sigma_g = \sqrt{\tilde{U}_{x,t_0}} = \bar{z}(n) \qquad (43)$$

It can be considered to be reachable either by exposure to patches of continuous turbulence of a certain duration or determined by repeated stochastic simulations comprised of a certain number n of time steps. For the latter, the number of time steps would be dependent upon the typical system dynamics and the duration of typical patches of continuous turbulence being simulated. Although not confirmed in this paper, the value of $\bar{z}$ determined for an uncorrelated sequence of values of the random quantity should serve as an upper bound on the peak-to-rms ratio for any physical linear system. What relationship, if any, the value of Eq. (43) would have to the peak-to-rms response of a nonlinear system cannot be stated in general.

While the preceding discussion explains the likely source of the peak-to-rms load ratio of around 3 for stochastic simulation, it is not immediately obvious how ratios of similar value were obtained for linear problems in Refs. 16 and 17. In these references, standard exceedance relationships and the probability densities of storm and nonstorm rms turbulence intensities that have been established for the atmosphere[13] were used. These probability densities were derived from extensive in-flight measurements of turbulence encounters. Regardless of how the measurements were made, the reduction of the data to generate the probability densities involved time discretization. Thus, the measured data become indistinguishable from the results of a stochastic simulation performed with a digital computer. In addition, the atmosphere is not unlike a digital random number generator to the extent that neither is going to actually produce an extremely large value (approaching infinity) of the random variable in question (intensity or gust velocity in the case of turbulence). Hence, it is possible that the derived probability structure of atmospheric turbulence, such as was used in Refs. 16 and 17, is influenced by data reduction in the same way as peak-to-rms ratios are affected by stochastic simulation using digital computers.

Conclusions

A description of the MFT interpretation of the maximum and time-correlated linear aircraft gust loads problem has been presented in this paper. The mathematical development is cast in terms of fundamental random process theory. It was shown that the energy of the excitation waveform is central to the determination of the magnitude of the maximum load, and can be related to the design gust velocity and load peak-to-rms ratio used in standard gust loads analyses. Within the same formalism, it was shown using extremal distributions of uncorrelated sequences of random events, that the maximum load obtained in stochastic simulations of gust loading performed with digital computers is dependent upon the number of time steps used in the simulation. Also, for reasonable simulation times, the load peak-to-rms ratio is near 3, at least for linear systems.

Further investigation of extremal distributions should be conducted that account for varying degrees of correlation between the events in random sequences. Also, the degree to which discretization of data has influenced the statistical descriptions of atmospheric turbulence is worthy of review.

References

[1]Jones, J. G., "Statistical Discrete Gust Theory for Aircraft Loads," Royal Aircraft Establishment, TR 73167, Nov. 1973.

[2]Perry, B., III, Pototzky, A. S., and Woods, J. A., "NASA Investigation of a Claimed "Overlap" Between Two Gust Response Anal-

ysis Methods," *Journal of Aircraft*, Vol. 27, No. 7, 1990, pp. 606–611.

[3]Pototzky, A. S., Zeiler, T. A., and Perry, B., III, "Calculating Time-Correlated Gust Loads Using Matched Filter and Random Process Theories," *Journal of Aircraft*, Vol. 28, No. 5, 1991, pp. 346–352.

[4]North, D. O., "Analysis of the Factors Which Determine Signal/Noise Discrimination in Radar," RCA Labs., RCA PTR-6C, Princeton, NJ, June 1943; also *Proceedings of the IEEE*, Vol. 51, July 1963, pp. 1016–1027.

[5]Zeiler, T. A., and Pototzky, A. S., "On the Relationship Between Matched Filter Theory as Applied to Gust Loads and Phased Design Loads Analysis," NASA CR 181802, April 1989.

[6]Scott, R. C., Pototzky, A. S., and Perry, B., III, "Determining Design Gust Loads for Nonlinear Aircraft — Similarity Between Methods Based on Matched Filter Theory and on Stochastic Simulation," NASA TM 107614, April 1992.

[7]Scott, R. C., Pototzky, A. S., and Perry, B., III, "Computation of Maximized Gust Loads for Nonlinear Aircraft Using Matched-Filter-Based Schemes," *Journal of Aircraft*, Vol. 30, No. 5, 1993, pp. 763–768.

[8]Scott, R. C., Pototzky, A. S., and Perry, B., III, "Matched-Filter and Stochastic-Simulation-Based Methods of Gust Loads Prediction," *Journal of Aircraft*, Vol. 32, No. 5, 1995, pp. 1047–1055.

[9]Carlson, A. B., *Communication Systems*, McGraw–Hill, New York, 1968.

[10]Papoulis, A., "Maximum Response with Energy Constraints and the Matched Filter Principle," *IEEE Transactions on Circuit Theory*, Vol. CT-17, No. 2, 1970, pp. 175–182.

[11]Peebles, P. Z., Jr., *Probability, Random Variables, and Random Signal Principles*, McGraw–Hill, New York, 1987.

[12]Stratonovich, R. L., "Optimum Nonlinear Systems for Isolating a Signal with Constant Parameters from Noise," *Nonlinear Transformations of Stochastic Processes*, edited by P. I. Kuznetsov, R. L. Stratonovich, and V. I. Tikhonov, translation edited by J. Wise and D. C. Cooper, Pergamon, Oxford, England, UK, 1965.

[13]"Continuous Gust Design Criteria," Airworthiness Standards: Transport Category Airplanes, Federal Aviation Regulations, Pt. 25, Appendix G, 1980.

[14]Moon, R. M., "A Summary of Methods for Establishing Airframe Design Loads from Continuous Gust Design Criteria," 65th AGARD Structures and Materials Panel, Turkey, Oct. 1987.

[15]Gould, J. D., "Effects of Active Control System Nonlinearities on the L-1011-3 (ACS) Design Gust Loads," AIAA Paper 85-0755, April 1985.

[16]Vinnecombe, G., Hockenhull, M., and Dudman, A. E., "Gust Analysis of an Aircraft with Highly Non-Linear Systems Interaction," 1989 Gust Specialists Meeting, Mobile, AL, April 1989.

[17]Noback, R., "S.D.G., P.S.D, and the Nonlinear Airplane," National Aerospace Lab., MP 88018 U, The Netherlands, April 1988.

[18]Gumbel, E. J., and Carlson, P. G., "Extreme Values in Aeronautics," *Journal of the Aeronautical Sciences*, Vol. 21, No. 6, 1954, pp. 389–398.